In situ STXM investigations of pentacene-based OFETs during operation

C. Hub,*[a] M. Burkhardt,[b] M. Halik,[b] G. Tzvetkov†[a] and R. Fink*[a]

Received 15th February 2010, Accepted 13th April 2010
First published as an Advance Article on the web 4th May 2010
DOI: 10.1039/c0jm00423e

Ultrathin pentacene-based organic field-effect transistors (OFETs) on commercially available silicon nitride membranes suitable for transmission X-ray experiments are demonstrated. The devices produced by high-vacuum deposition show excellent electronic performance ($\mu = 0.6$ cm^2 V^{-1} s^{-1}, $I_{on/off} = 10^6$). STXM-experiments recorded with the PolLux microspectroscope correlate structural and electronic properties at highest spatial and spectral resolution while the OFET is operated. Local NEXAFS spectra are used to analyze the different orientations of the pentacene nanocrystals. Spectral changes due to modifications in the electronic structure during OFET operation can hardly be detected with the current setup.

Introduction

Remarkably improved performance by research efforts of uncounted groups opened the way to commercial applications of organic semiconductors.[1–3] Based on a better understanding and improved control of the film growth, organic semiconducting devices have reached the performance of amorphous silicon products.[4,5] Nevertheless, the comparison of polycrystalline thin film devices to the electronic performance of devices based on organic single crystals shows that there is still plenty of room for further improvement.[6,7] It is well established that the polycrystalline morphology affects the transport characteristics in organic thin film devices. However, imaging techniques like, *e.g.*, atomic-force microscopy (AFM) can hardly offer insight into individual nano- or microdomains.

In this paper we report on the investigation of thin film organic field-effect transistors (OFETs) with emphasis on the correlation of morphological and electronic properties using scanning transmission soft X-ray microspectroscopy (STXM). Due to the limited penetration depth of soft X-rays ultrathin film samples are required. Therefore, we prepared our OFET devices on commercially available ultrathin Si_3N_4 membranes. This in contrast to many other pentacene-based OFETs reported in the literature where thin film dielectrics on solid substrate crystals are used.[5,8–10]

STXM relies on the near-edge X-ray absorption fine structure (NEXAFS/XANES) contrast by probing the unoccupied states when a focused X-ray beam is raster-scanned across the sample. Several contrast mechanisms, *e.g.*, thickness modulations or chemical and elemental contrast due to photon energy dependent absorption, are suitable to record an image of a thin film sample. In the present devices only carbon K-edge absorption needs to be considered. At energies well above the K absorption edge of carbon (>318 eV) the difference in absorption intensities is purely based on thickness and density variations within the film. At the respective absorption resonances, the linear absorption dichroism may be applied to deduce the molecular orientation.[11]

Besides the characterization of the transport properties and the microscopic imaging of thus prepared OFETs, we are considering the possibility of identifying changes in the electronic properties while the OFET is operated. Applying a gate voltage and driving a current through the device will induce changes in the electronic levels, which should be accessible by means of core-electron excitation spectroscopy.

Experimental

The thin film devices were prepared by subsequent deposition of the different materials (pentacene, gold contacts) through a shadow mask under high-vacuum conditions ($p < 1 \times 10^{-6}$ mbar) in the so-called top-contact geometry [Fig. 1(a)]. As dielectric, commercially available Si_3N_4 membranes (thickness: 100 nm; membrane size: 1×1 mm^2; supplier: Silson Ltd., UK) were used. On the backside of the dielectric an aluminium film with a nominal thickness of 20 nm was deposited at a rate of 1 Å s^{-1} as gate contact.

Pentacene purchased from Sigma Aldrich and resublimed twice prior to film deposition was used as active organic semiconducting material. Nominally 30 nm thick pentacene films were grown at a rate of 0.1 Å s^{-1} at 333 K as controlled by a quartz microbalance (base pressure: $<5 \times 10^{-7}$ mbar). After evaporation the samples were held at 333 K for another two hours and stored in vacuum over night to ensure the formation of a high quality pentacene film. The devices have a channel width $W = 250$ μm and a length $L = 40$ μm (W/L ratio: 6.25) or $L = 20$ mm (W/L ratio: 12.5), respectively.

We have chosen Au top electrodes (thickness 30 nm) due to their low injection barrier[12] to achieve maximum electronic performance. Thus, the overall device thickness is thin enough to allow sufficiently high transmittance for soft X-rays which are used for high spatial resolution electron microspectroscopy in STXM. The analysis of metal–insulator–metal (MIM)-structure

[a]*Department Chemistry and Pharmacy and Interdisciplinary Center for Molecular Materials (ICMM), Friedrich-Alexander Universität Erlangen-Nürnberg, Egerlandstraße 3, 91058 Erlangen, Germany. E-mail: christian.hub@chemie.uni-erlangen.de; rainer.fink@chemie.uni-erlangen.de*
[b]*Institute of Polymer Materials, Friedrich-Alexander Universität Erlangen-Nürnberg, Martensstraße 7, 91058 Erlangen, Germany*
† Permanent address: Department of Inorganic Chemistry, University of Sofia, 1164 Sofia, Bulgaria.

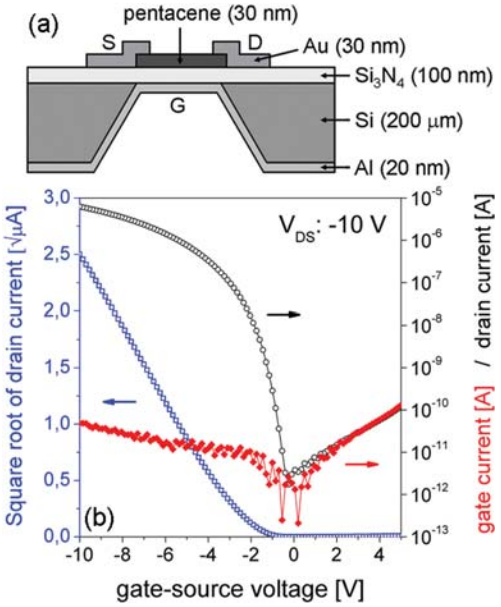

Fig. 1 (a) Schematic drawing of the prepared top-contact, bottom-gate (Al, 20 nm) thin film OFETs and (b) the resulting electric properties. Source (S)–drain (D) voltage was −10 V for the presented data.

devices revealed an average dielectric strength of 12.3 MV cm^{-1}, a dielectric constant of $\varepsilon_r = 9.89$ and an area capacitance of 87.5 nF cm^{-2} for our silicon nitride dielectric. For device operation a negative gate voltage (V_{GS}: −10 V) was applied. The electrical characteristics of the devices were recorded with an Agilent 4156C parameter analyser under ambient conditions at room temperature.

Our STXM experiments were performed at the PolLux STXM at the Paul Scherrer Institut (PSI, Villigen, Switzerland), which has proven spatial resolutions as low as 20 nm.[13–15] Zone-plate focusing is used to achieve 40 nm lateral resolution in routine operation.[13] The photon energy dependent absorption signal (I_t/I_0) is measured by a conventional photomultiplier detector mounted behind the sample from comparison of the transmitted intensity (I_t) with the incoming photon flux (I_0).

Results

The electrical transfer characteristics of a selected device are shown in Fig. 1(b). A maximum gate current of 48 pA (filled diamonds, leakage at U_{GS}: −10 V) was obtained. Extracted from the saturation regime of the $\sqrt{I_{DS}}$ *vs.* V_{GS} plot, also included in Fig. 1(b) (open squares), the charge carrier mobility was determined to be 0.35 $cm^2 V^{-1} s^{-1}$ and the threshold voltage as −2.3 V. In addition, our devices exhibit a subthreshold slope of 0.3 V dec^{-1} and the on/off current ratio is as large as 10^6. Thus, the electronic properties of our devices are compatible with recently published data of state-of-the-art pentacene OFETs.[16]

Two STXM micrographs, presented in Fig. 2, show an area of the pentacene film within the channel of the source and drain electrodes. A photon energy of 320 eV was used to record the image of Fig. 2(a). At this energy no particular spectral features appear for pentacene. Thus, the transmitted intensity reflects the thickness dependence and the modulation in the image is due to morphology variations in the film. The image recorded at 285.8

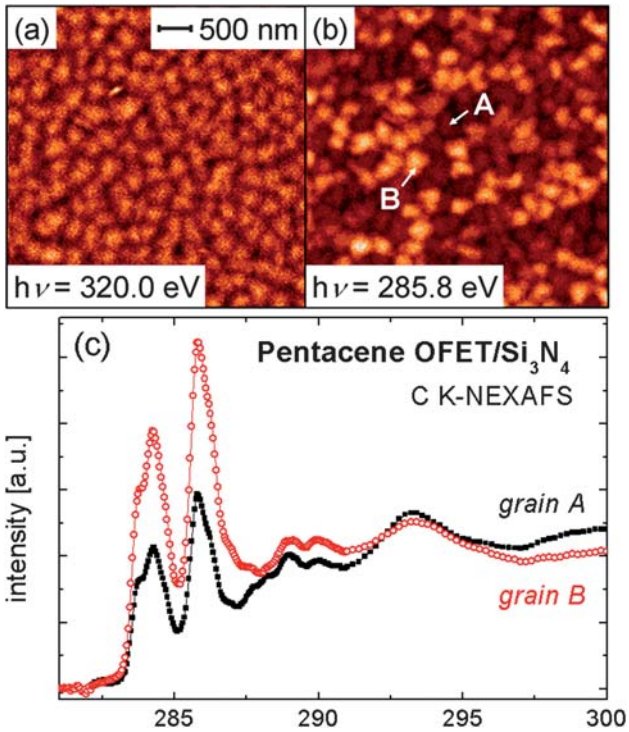

Fig. 2 Scanning soft X-ray transmission micrographs of the prepared pentacene films (nominal thickness: 30 nm) recorded at photon energies of 320 eV (a) and 285.8 eV (b), respectively (scanned area: 5 × 5 μm^2), and (c) C K-edge NEXAFS spectra extracted from two selected grains. From the relative intensity changes the average tilt angle of the molecules within the grains may be derived (see text).

eV [Fig. 2(b)], which corresponds to the main C 1s absorption resonance of pentacene,[17] shows higher contrast compared to Fig. 2(a). A relatively homogenous size distribution with an average diameter of the individual pentacene grains of around 250 nm was found. It is well known that the actual size distribution and homogeneity of the organic film strongly depend on the preparation conditions and strongly affect the electronic performance of the devices, *e.g.*, the charge carrier mobility, which is discussed controversially in the current literature.[18,19]

In order to explore the intensity differences in more detail, local NEXAFS spectra from the two adjacent grains marked A and B in Fig. 2(b) were recorded. The extracted spectra shown in Fig. 2(c) were normalized to the pre- (280 eV) and post-absorption edges (320 eV) according to standard procedures.[11] Simplified, the resonances originate from the excitation of a localized core electron into unoccupied delocalized molecular orbitals (π*) or quasi-bound vacuum states (σ*). The absorption signal strongly depends on the polarization of the incident photons with respect to the unoccupied molecular orbitals.[11] In C K-NEXAFS of pentacene, the most intense and sharp π*-resonances may be used to derive the molecular orientation. The NEXAFS resonances of pentacene have been discussed in several publications and shall not be considered here.[17,20,21] For the present discussion only the intensity differences of the π*-resonances in the energy range from 282.5 to 289 eV are relevant. The intensity in the two representative grains differs by more than a factor of 2 in the normalized spectra which is unambiguously attributed to differences in the respective grain orientations.

For a more detailed analysis of the dichroism a rotational device (see Hernández-Cruz *et al.*[22]) was implemented into the PolLux microspectroscope. X-Ray micrographs recorded at different azimuthal orientations ($\alpha = 0°$, 25°, 50°) are presented in Fig. 3(a)–(c). Again a polycrystalline film consisting of coalescing grains with differently orientated molecular unit cells is found. Within the presented images two representative areas are highlighted. In these highlighted areas even a contrast reversal for selected grains can be easily observed while the specimen is rotated.

The determination of their absolute orientations is not straightforward, since no preferential azimuthal angle is accessible from the present data and, in addition, the polarization of the incoming radiation cannot be rotated in the present STXM setup to explore the full angular dependence. However, additional AFM investigations of monolayer films on the silicon nitride substrates (not shown here) revealed a monolayer film thickness of approximately 1.6 nm that perfectly fits to the length of a single pentacene molecule. Therefore, we can conclude that the pentacene molecules are standing upright on our silicon nitride substrate (or only slightly deviating from perpendicular orientation). In addition, if we assume the observed thin film phase found for pentacene on silicon dioxide,[23–25] each unit cell contains two molecules. Unfortunately it is not possible to determine the exact angle that is spanned by the molecular planes of these two molecules within the unit cell by STXM microscopy. Assuming a perpendicular (or almost perpendicular) long-axis molecular orientation in grain B in Fig. 2(b), we estimated a relative difference of azimuthal rotation of about 30 degrees for grain A. Exact determination would require additional experiments with significant out-of-plane polarization of the X-rays (with respect to the sample substrate), which cannot be performed in the present PolLux-STXM setup.

The third aspect of this paper concerns the changes in the electronic structure while the OFET devices are operated. It is well established that the majority of the charge carriers are located within the first few monolayers to the dielectric.[20,26] To get access to this accumulation layer and to improve the signal to background ratio ultrathin pentacene films are essential. Therefore, pentacene OFET devices with a nominal thickness of 7 nm (confirmed with atomic force microscopy) with sufficient electronic performance ($\mu = 0.03$ cm^2 V^{-1} s^{-1}, $I_{on/off} = 10^5$) were prepared. C K-NEXAFS spectra of the pentacene film recorded in the area between the source and drain contacts for different gate–source and drain–source voltages are shown in Fig. 4. The

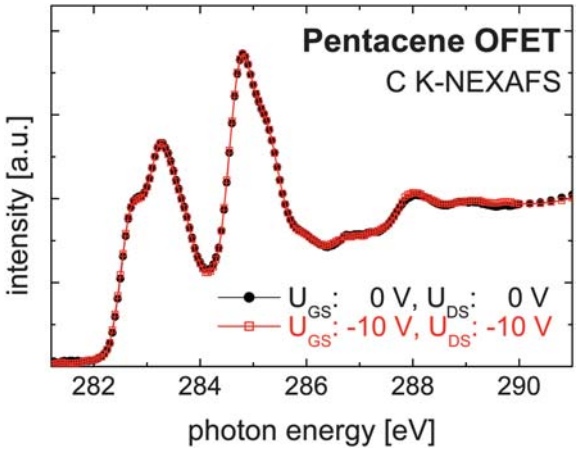

Fig. 4 C K-NEXAFS spectra of the pentacene OFET/Si_3N_4 for the on- (open squares) and off-status (filled circles) recorded in the transport channel between the source and drain contact of the 7 nm pentacene device.

spectral signatures of the low-energy spectral region resemble those of Fig. 2(c), *i.e.* spectrum of grain A. A similar film morphology as in the 30 nm device was found (not shown here) and intensity variations are again due to different azimuthal orientations. For on- and off-states no pronounced differences are detected, *i.e.*, according to the local NEXAFS spectra no change in the (overall) electronic structure occurs (valid for the 7 nm and 30 nm devices as well), which shall be discussed below.

Discussion and conclusions

In this paper we have presented transport data for pentacene-based OFETs prepared on freestanding ultrathin commercial Si_3N_4 membranes which allow *in situ* electronic structure analysis in high-resolution STXM. Si_3N_4 thin films on Si wafers have previously been used as dielectric for pentacene OFETs by Knipp *et al.*[27] With pentacene thicknesses of 50–70 nm prepared at higher sublimation rates and substrate rms-values of 0.5 nm, their transport characteristics and on/off-ratios of up to 10^8 are close to the ones reported here. Of course with increased nominal film thicknesses the rms-values may improve thus explaining the slightly higher on/off-ratios reported in ref. 27.

Our present STXM experiments give clear indications that the pentacene films are polycrystalline with much larger rms-values when investigated on longer length scales compared to

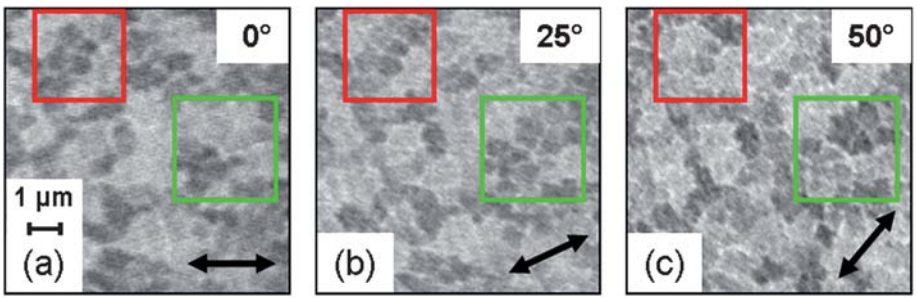

Fig. 3 STXM micrographs of a nominally 30 nm pentacene film prepared on Si_3N_4 membranes. For the individual images, the electric field vector (↔) is rotated by 0° (a), 25° (b), and 50° (c), respectively, resulting in different absorption probabilities, as indicated by the intensity variations in the highlighted squares.

conventional AFM topography analysis. Standard X-ray absorption investigations of thin pentacene films report on average tilt angles of 11 degrees with respect to the surface normal for pentacene on SiO_2 substrates.[24] For metal substrates the much larger interaction at the metal–pentacene interface leads to coplanar orientation of the aromatic system which relaxes to bulk-like orientation similar to SiO_2.[17] We should, however, point out that conventional NEXAFS averages over areas of about 1 mm^2 and may therefore not resolve orientation inhomogeneities as in STXM. Our present studies indicate that the grains with different azimuthal orientations may affect the transport properties in the ultrathin polycrystalline films.

Finally, we would like to address the aspect, why our present NEXAFS studies cannot detect changes in the electronic structure while the OFET is operated. Additional charges on the pentacene molecules would implement changes in the molecular orbitals, *i.e.*, one expects either differential energetic shifts of the NEXAFS resonances or variations in the NEXAFS intensities due to additional draining (accumulation of holes) of the molecular orbitals. Moreover, a polarization within the upright standing pentacene molecules is induced by the electric field of the gate bias. This polarization is expected to lead to an energetic shift of the involved HOMO and LUMO electronic states.

Several aspects may be considered to explain the missing spectral changes in the present experiments. First, calculation of the area charge Q within the channel of our devices revealed that only about one percent of the pentacene molecules carries electric charge.[28] Second, as in STXM the transmitted intensity is detected, it is mainly sensitive to the bulk signal of the pentacene film. However, the majority of the charge transport takes place within the first few nanometres of the film.[26,29] Thus, signals originating from the pentacene–dielectric interface are recorded against a relatively large background signal originating from photons, that were not absorbed within the film, while the major absorption stems from the bulk material. A signal change (intensity damping or spectral shift) originating from 10–20 percent of the molecules within the whole film should be expected.‡ Another argument for the missing spectral changes during on/off-operation may be the insensitivity of the core-excitations due to very short-lived excitonic-states in polarized molecules. However, since the excitations occur on the timescale of 10^{-17} s, we do not expect such ultrafast relaxation processes. More probably is a potential Fermi-level pinning that has been discussed for the pentacene–SiO_2 interface.[30] In that case, no spectral changes at the low-energy onset of the NEXAFS spectra are to be expected.

Future developments may, however, improve the thin-film sensitivity of STXM, in particular when electron yield detection using channeltron detectors is employed.[14] Pentacene-based OFETs with film thicknesses of 5 nm and good device characteristics have successfully been prepared. Such devices may be used to finally observe local modifications to the electronic structure if no other than the above mentioned effects apply.

‡ This estimation is based on an average film thickness of about 4 monolayers and, in addition, dichroic effects, *i.e.* dependence of absorption on azimuthal orientations of the individual grains.

Acknowledgements

The authors acknowledge financial support from the BMBF (contract 05KS7WE1) and ICMM. We would like to thank B. Graf, St Wenzel and Dr J. Raabe for experimental support. The PolLux end station was financed by the BMBF (contract 05KS4WE1/6). M.B. would like to thank the Cluster of Excellence "Engineering of Advanced Materials" (EAM).

References

1 G. Horowitz, *J. Mater. Res.*, 2004, **19**, 1946–1962.
2 M. Ahles, R. Schmechel and H. von Seggern, *Appl. Phys. Lett.*, 2005, **87**, 113505.
3 P. Mach, S. J. Rodriguez, R. Nortrup, P. Wiltzius and J. A. Rogers, *Appl. Phys. Lett.*, 2001, **78**, 3592–3594.
4 H. Klauk, *Organic Electronics: Materials, Manufacturing and Applications*, Wiley-VCH, Weinheim, 2006.
5 C. D. Dimitrakopoulos and P. R. L. Malenfant, *Adv. Mater.*, 2002, **14**, 99–117.
6 V. C. Sundar, J. Zaumseil, V. Podzorov, E. Menard, R. L. Willett, T. Someya, M. E. Gershenson and J. A. Rogers, *Science*, 2004, **303**, 1644–1646.
7 R. W. I. de Boer, M. E. Gershenson, A. F. Morpurago and V. Podzorov, *Phys. Status Solidi A*, 2004, **201**, 1302–1331.
8 S. F. Nelson, Y.-Y. Lin, D. J. Gundlach and T. N. Jackson, *Appl. Phys. Lett.*, 1998, **72**, 1854–1856.
9 H. Klauk, M. Halik, U. Zschieschang, G. Schmid and W. Radlik, *J. Appl. Phys.*, 2002, **92**, 5259–5263.
10 M. J. Panzer, C. R. Newman and C. D. Frisbie, *Appl. Phys. Lett.*, 2005, **86**, 103503.
11 J. Stöhr, *NEXAFS Spectroscopy*, Springer Verlag, Berlin, 1992.
12 S. Rentenberger, A. Vollmer, E. Zojer, R. Schennach and N. Koch, *J. Appl. Phys.*, 2006, **100**, 053701.
13 J. Raabe, G. Tzvetkov, U. Flechsig, M. Böge, A. Jaggi, B. Sarafimov, M. G. C. Vernooij, T. Huthwelker, H. Ade, D. Kilcoyne, T. Tyliszczak, R. H. Fink and C. Quitmann, *Rev. Sci. Instrum.*, 2008, **79**, 113704.
14 C. Hub, S. Wenzel, J. Raabe, H. Ade and R. Fink, *Rev. Sci. Instrum.*, 2010, **81**, 033704.
15 K. Jefimovs, J. Vila-Comamala, T. Pilvi, J. Raabe, M. Ritala and C. David, *Phys. Rev. Lett.*, 2007, **99**, 264801.
16 N. Koch, *ChemPhysChem*, 2007, **8**, 1438–1455.
17 S. Lukas, S. Söhnchen, G. Witte and C. Wöll, *ChemPhysChem*, 2004, **5**, 266–270.
18 H. Yanagisawa, T. Tamaki, M. Nakamura and K. Kudo, *Thin Solid Films*, 2004, **464**, 398–402.
19 W. Kalb, P. Lang, M. Mottaghi, H. Aubin, G. Horowitz and M. Wuttig, *Synth. Met.*, 2004, **146**, 279–282.
20 F. Zheng, B.-N. Park, S. Seo, P. G. Evans and F. J. Himpsel, *J. Chem. Phys.*, 2007, **126**, 154702.
21 H.-K. Lee, J.-H. Han, K.-J. Kim, T.-H. Kang and B. Kim, *Surf. Sci.*, 2007, **601**, 1456–1460.
22 D. Hernández-Cruz, A. P. Hitchcock, T. Tyliszczak, M.-E. Rousseau and M. Pézolet, *Rev. Sci. Instrum.*, 2007, **78**, 033703.
23 C. D. Dimitrakopoulos, A. R. Brown and A. Pomp, *J. Appl. Phys.*, 1996, **80**, 2501–2508.
24 S. E. Fritz, S. M. Martin, C. D. Frisbie, M. D. Ward and M. F. Toney, *J. Am. Chem. Soc.*, 2004, **126**, 4084–4085.
25 R. Ruiz, D. Choudhary, B. Nickel, T. Toccoli, K.-C. Chang, A. C. Mayer, P. Clancy, J. M. Blakely, R. L. Headrick, S. Iannotta and G. G. Malliaras, *Chem. Mater.*, 2004, **16**, 4497–4508.
26 E. L. Granstrom and C. D. Frisbie, *J. Phys. Chem. B*, 1999, **103**, 8842–8849.
27 D. Knipp, R. A. Street and A. R. Völkel, *Appl. Phys. Lett.*, 2003, **82**, 3907–3909.
28 R. Schmechel, M. Ahles and H. von Seggern, *J. Appl. Phys.*, 2005, **98**, 084511.
29 P. Zhang, E. Tevaarwerk, B. N. Park, D. E. Savage, G. K. Celler, I. Knezevic, P. G. Evans, M. A. Eriksson and M. G. Lagally, *Nature*, 2006, **439**, 703–706.
30 L. Chen, R. Ludeke, X. Cui, A. G. Schrott, C. R. Kagan and L. E. Brus, *J. Phys. Chem. B*, 2005, **109**, 1834–1838.